

## Numerical Analysis on Melting and Solidification of Pure Metals with Enthalpy-Porosity Model

Sin Kim, Bum Jin Chung and Min Chan Kim\*

*Department of Nuclear and Energy Engineering*

*\*Department of Chemical Engineering, Cheju National University*

**Abstract** — A finite volume numerical approach is developed and used to simulate convection-dominated melting and solidification problems. The present approach is based on the enthalpy-porosity method that is traditionally used to track the motion of the liquid-solid front and to obtain the temperature and velocity profiles in the liquid-phase. The enthalpy-porosity model treats the solid-phase as the porosity in all computational cells that are located on the solid-liquid interfacial boundary. Concerning the computational cells that are fully located in the solid side of the interfacial boundary, the zero value of the porosity severely suppresses the velocity vector to practically a non-existent value that could be set equal to zero. A comparative analysis with the previous numerical approaches is performed to demonstrate the improved features of the presented model. Results of a melting and solidification experiments are also used to assess and evaluate the performance of the model.

### 1. Introduction

In many engineering fields such as thermal energy storage systems using latent heat and materials processing, the melting and solidification is an important process. The temperature difference in the melt can give rise to the natural convection. Also, the flow structure can significantly affect the phase change process. The convection greatly influences the morphology of the solid-liquid interface by changing the flow structure in the melt.

In general, numerical simulations commonly used for phase change problem are classified into two different approaches: the fixed-grid and the transformed-grid methods. The fixed-grid method uses a single set of conservation equations and boundary conditions for the whole domain comprising the solid and liquid phases, while the transformed-grid method employs the governing equations based on the classical Stefan formulation. The interface conditions, therefore, are accounted for differently according to the method incorporated in solving the phase change problem. In the transformed-grid method, they are easily imposed because the interface is explicitly solved. However, in the fixed-grid method, the interface conditions are described as suitable source terms in the governing equations. A

nodal latent heat value is assigned to each computational cell according to its temperature or enthalpy. Upon phase changing, the latent heat absorption, or evolution, is reflected as a source, or sink, term in the energy equation.

The fixed-grid method requires the velocity suppression because as a liquid region turns solid, the zero-velocity condition should be satisfied. The velocity suppression can be accomplished by a large value of viscosity for the solid phase or by a suitable source term in the momentum equation to model the two-phase domain as a porous medium. The fixed-grid method combined with the porous medium method is usually referred to as the enthalpy-porosity method.

To simulate the phase change process, this paper proposes a simple numerical scheme based on the enthalpy-porosity method. The numerical results are verified with the experimental data. A comparative analysis with the finite volume and the finite element approaches is performed. Also, the effect of the interpolation scheme for the convection term on the numerical results is analyzed.

The spatial and temporal discretizations are achieved in the context of the finite volume scheme and the fully implicit (backward) Euler scheme, respectively.

The flow field is expressed in terms of primitive variables and solved by adopting SIMPLE algorithm.

## 2. Mathematical Models for Convection-Dominated Phase Change Problems

The momentum field is subjected to no-slip boundary conditions at the walls. The flow is assumed to be two-dimensional, laminar, and incompressible. The physical properties of the material are constant, but may differ for the liquid and solid phases. The density difference between solid and liquid phases is negligible except when utilizing the Boussinesq approximation.

In the fixed-grid method, the absorption and evolution of the latent heat during phase change leads to the modification of the energy equation because the interface is not tracked, and thus the interface conditions are not imposed explicitly. The fixed-grid method relies on the enthalpy formulation, which employs the enthalpy as a dependent variable in the energy equation rather than the temperature. The enthalpy formulation defines the liquid mass fraction  $f$  as the ratio of the liquid mass to the total mass in a given computational cell. If  $h_s$  and  $T_m$  are set to the reference enthalpy (e.g. saturation enthalpy of solid phase) and temperature (e.g. melting temperature), respectively, the specific enthalpy will be

$$h = fL + cT. \quad (1)$$

The latent heat and the heat capacity are denoted by  $L$  and  $c$ , respectively. The heat capacity  $c$  may vary with the phase. The liquid mass fraction can be obtained from the enthalpy:

$$f = \begin{cases} 0 & \text{if } h < 0 \\ \frac{h}{L} & \text{if } 0 \leq h \leq L \\ 1 & \text{if } L < h \end{cases} \quad (2)$$

In isothermal phase change with stationary solid phase, the following enthalpy-based governing equations are obtained:<sup>[1]</sup>

$$\frac{\partial u}{\partial x} + \frac{\partial v}{\partial y} = 0, \quad (3)$$

$$\rho \left( \frac{\partial u}{\partial t} + u \frac{\partial u}{\partial x} + v \frac{\partial u}{\partial y} \right) = -\frac{\partial p}{\partial x} + \mu \left( \frac{\partial^2 u}{\partial x^2} + \frac{\partial^2 u}{\partial y^2} \right) + S_u, \quad (4a)$$

$$\rho \left( \frac{\partial v}{\partial t} + u \frac{\partial v}{\partial x} + v \frac{\partial v}{\partial y} \right) = -\frac{\partial p}{\partial y} + \mu \left( \frac{\partial^2 v}{\partial x^2} + \frac{\partial^2 v}{\partial y^2} \right) + \rho g \beta (T - T_{ref}) + S_v, \quad (4b)$$

$$\rho \left[ \frac{\partial}{\partial t} (cT) + u \frac{\partial}{\partial x} (cT) + v \frac{\partial}{\partial y} (cT) \right] = k \left( \frac{\partial^2 T}{\partial x^2} + \frac{\partial^2 T}{\partial y^2} \right) - \rho L \frac{\partial f}{\partial t}. \quad (5)$$

In these equations,  $S_u$  and  $S_v$  are source terms to account for the velocity suppression.

During the solution process of the momentum field, the velocity at the computational cell located in the solid phase should be suppressed while the velocities in the liquid phase remain unaffected. One of the popular models for the velocity suppression is to introduce a Darcy-like term:<sup>[1]</sup>

$$S_u = -C \frac{(1-f)^2}{(f^3+b)} u \quad \text{and} \quad S_v = -C \frac{(1-f)^2}{(f^3+b)} v \quad (6)$$

which is easily incorporated into the momentum equation as shown in Eq. (4). The constant  $C$  has a large value to suppress the velocity as the cell becomes solid and  $b$  is a small number used to prevent the division-by-zero when a cell is fully located in the solid region, namely  $f=0$ . The choice of the constants is arbitrary. However, the constants should ensure sufficient suppression of the velocity in the solid region and should not influence the numerical results significantly. In this work,  $C=1 \times 10^9 \text{ kg/m}^3 \text{ s}$  and  $b=0.005$  are used.<sup>[1]</sup>

## 3. Numerical Methods

The SIMPLE algorithm<sup>[2]</sup> is employed to determine the velocity and pressure field. The power scheme<sup>[2]</sup> and the deferred correction method<sup>[3]</sup> are introduced in the interpolation scheme for the convection term. In the deferred correction, the lower-order flux approximation is implicitly imposed while the higher-order approximation is explicitly obtained from the previous iteration. For example, the flux through the east face,  $F_e$ , is represented as

$$F_e = F_e^l + \gamma (F_e^H + F_e^l)^{old} \quad (7)$$

where the superscript 'H' and 'L' denote the higher- and the lower-order approximation and  $\gamma$  is the blending factor to mix the two schemes. Normally, the explicit part is so small that it may not affect the convergence significantly. In this study, as the lower- and the higher-order scheme, the upwind difference scheme and the central difference scheme are chosen, respectively. The case with  $\gamma=0.5$  is referred as the mixed difference scheme.

The discretized energy equation in the finite volume formulation<sup>[2]</sup> can be expressed as

$$a_p T_p = \sum_{nb} a_{nb} T_{nb} + S_p - a_p^0 (f_p - f_p^*) \quad (8)$$

where subscripts 'P' and 'nb' refer to the value of present and neighboring cell, respectively. Superscript '\*' denotes the value at previous time step. The detailed expressions of the influence coefficients  $a_p$ ,  $a_{nb}$ ,  $a_p^0$  and source term  $S_p$  can be determined easily (refer Ref. [2]). The terms relating to the liquid fraction separate the non-linear behavior associated with the phase change into a source term.

If the discretized equation Eq. (8) is solved properly at the n-th iteration step, the enthalpy obtained with physical properties assumed at the n-th iteration step satisfies the energy conservation. Then, the enthalpy and the liquid fraction can be obtained from Eqs. (1) and (2), respectively. This procedure enables the energy contained in the cell to redistribute so that the excessive (or deficient) energy can be stored into (or retrieved from) latent heat rather than spurious sensible heat. Also, the temperature can be re-estimated according to the new mass fraction

$$T_p^{(n+1)} = \left( \frac{h^{(n+1)}}{L} - f^{(n+1)} \right) \frac{L}{c^{(n+1)}} \quad (9)$$

which gives a better estimation of the temperature for the next iteration.

At the phase changing cell, the updated temperature distribution should satisfy the discretization equation. If we assume the present cell 'P' is undergoing phase change, the temperature is given by

$$T_p^{(n+1)} = \frac{\sum_{nb} a_{nb}^{(n+1)} T_{nb}^{(n)} + GS_p^{(n+1)}}{a_p^{(n+1)}} \quad (10)$$

The generalized source  $GS_p$  can be easily obtained

from Eq. (8). The influence coefficients and the generalized source are calculated with the updated mass fraction  $f^{(n+1)}$ . Although the temperatures of neighboring cells  $T_{nb}$  are obtained at the previous iteration step and may be comparatively less correct than the other updated values, the new temperature  $T_p^{(n+1)}$  based on the updated mass fraction will be a more accurate estimation. This temperature can be used to update the mass fraction with the enthalpy expression. This predictor-corrector procedure will be applied iteratively only to phase changing cells consisting in the phase change front. The whole set of the governing equations do not need to be solved during this procedure. It should be noted that during the inner iteration, the temperatures at neighboring cells are not changed but the updated temperature is a good estimation for the next iteration. The proposed algorithm seems to be very effective due to its simplicity and low computational cost. Furthermore, this can be readily adaptable to any numerical scheme designed for computational efficiency. This algorithm always ensures the energy conservation at the phase changing cell.

In this study, another simple algorithm is introduced to further improve the convergence. Consider the predictor-corrector procedure used in the discretized energy equation, Eq. (8). During the procedure, in order to obtain the converged temperature faster from the non-linear relations, the Newton-Raphson method is employed. The problem will be to find the temperature that minimizes the objective function  $\Phi$ :

$$\Phi = a_p T_p - \left[ \sum_{nb} a_{nb} T_{nb} + S_p - a_p^0 (f_p - f_p^*) \right] \quad (11)$$

The updated temperature will be

$$T_p^{(n+1)} = T_p^{(n)} - \Phi^{(n)} \left[ \frac{\partial \Phi^{(n)}}{\partial T_p} \right]^{-1} \quad (12)$$

and if the Jacobian  $\partial \Phi / \partial T_p$  is known, the Newton-Raphson method can assure faster convergence. However, the Jacobian cannot be calculated cheaply.

Recalling that the neighboring temperatures are assumed to be constant during the predictor-corrector procedure and  $f$  does not have terms relating to  $T_p$  explicitly and assuming that the thermo-physical properties are not dependent on the temperature strongly, the Jacobian can be approximated as  $\partial \Phi^{(n)} / \partial T_p \cong a_p^{(n)}$ .

Therefore, the updated temperature will be easily obtained:

$$T_p^{(n+1)} = T_p^{(n)} - \frac{\Phi^{(n)}}{a_p^{(n)}} \quad (13)$$

Even though the Jacobian is not directly calculated, the preliminary studies on heat-conduction phase-change examples show that this Newton-Raphson like scheme reduces the total number of inner iterations required for converged solutions by 2/3 of the original one.<sup>[4]</sup>

#### 4. Numerical Results and Discussions

The convection-dominated melting of a pure gallium is simulated with the proposed algorithm. The numerical predictions are verified and discussed with the experimental and numerical results in the literature. The experiment of Gau and Viskanta<sup>[5]</sup> is men-

tioned as a reference because it has been widely cited for the verification of numerical models.<sup>[1][6]</sup> The present numerical results are compared with the transformed-grid results<sup>[1]</sup> and the finite element solutions.<sup>[6]</sup>

The experimental configuration is sketched in Fig. 1. Initially, a solid gallium block is kept at  $T_i=28.3^\circ\text{C}$ . The temperature at the left wall is increased instantly to  $38.0^\circ\text{C}$ , while the right wall is maintained at the initial temperature. The physical properties used in the calculation are adopted from Brent *et al.* (1988).<sup>[7]</sup>

The Prandtl number, the Rayleigh number and the Stefan number are defined as

$$Pr = \frac{\nu_l}{\alpha_l}, \quad Ra = \frac{g\beta\Delta TH^3}{\alpha_l\nu_l} \quad \text{and} \quad Ste = \frac{c_l(T_H - T_m)}{L} \quad (14)$$

thus,  $Pr=0.0216$ ,  $Ra=6.057 \times 10^5$  and  $Ste=0.03912$ , respectively. In this,  $T_m$  is the melting temperature,  $L$  is the latent heat,  $H$  is the cavity height and the temperature difference is defined as  $\Delta T=T_H-T_m$ . In the simulation, we use uniformly spaced  $50 \times 36$  grid, which is similar to the grid ( $50 \times 30$ ) adopted by Viswanath and Jaluria<sup>[1]</sup> after a grid sensitivity study.

The predicted phase change fronts are shown with the results from the experiment and other numerical models in Fig. 2. The convection term is interpolated based on the mixed difference scheme. When analyzing solid-liquid interfaces at 6 and 10 min, all numerical results calculated using these models are in agreement with the experimental data. At 19 min the solid-liquid interfaces obtained by the fixed-grid ap-

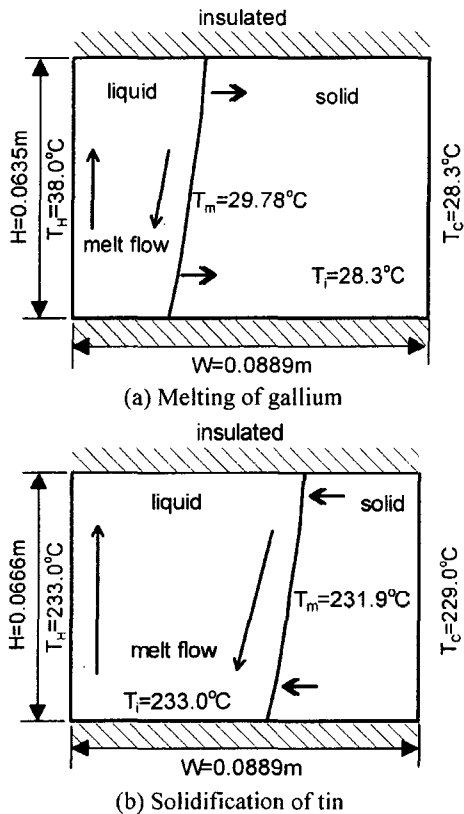


Fig. 1. Schematics of phase change problems in a rectangular cavity.

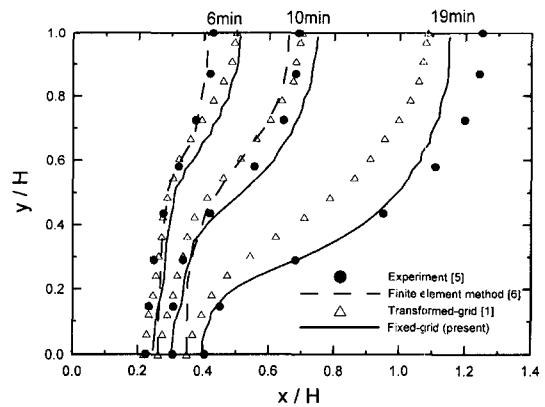


Fig. 2. Phase change fronts during the gallium melting.

proach show differing results than that of the experiment, especially at the top region. Such discrepancy may be attributed to several factors. Even though the hot wall temperature is assumed to reach the desired temperature upon starting the experiment, in fact, to raise the temperature impulsively to the desired one is very difficult in practice. The actual amount of energy transferred to the gallium through the hot wall should be less than that imposed in the idealized calculation, so that the retardation of the front evolution in experiments may be likely. The inaccurate modeling of the physical properties such as the anisotropic nature of the thermal conductivity, as well as, the numerical modeling error can be another reason of the discrepancy. At 19 min when the effect of delayed heat-up at the hot wall is less significant, the interfaces obtained with the fixed-grid correspond better than those with the transformed-grid. The finite element results at 19 min are not listed due to the lack of the data (Desai and Vafai, 1993).<sup>16)</sup>

In order to show the flow structure in the melt, the streamlines are plotted in Fig. 3. An interesting point to note is that the flow structures obtained in previous

studies<sup>7-10)</sup> show only a single cell in the melt region. With the transformed-grid, Viswanath and Jaluria<sup>11)</sup> observed a secondary recirculation cell in the lower part of the melt region. However, the secondary recirculation eddies are missed completely by the fixed-grid with the enthalpy method. They used the power scheme for the interpolation of the convection term. To analyze their effect on the numerical results, in the present study, we adopt 4 often-used interpolation schemes for the convection term: the upwind difference, the central difference, the mixed schemes and the power scheme. Even though the central difference scheme is known to suffer from severe oscillation on coarse grids, it converges more rapidly to an accurate solution as the grid is refined and offers a good compromise among accuracy, simplicity and efficiency as stressed by Ferziger and Peric.<sup>3)</sup> The central difference scheme predicts the secondary cell and the mixed difference scheme shows the obvious distortion of the streamlines in the lower melt region at 19 min. The power and the upwind difference schemes fail to predict the minor flow motion in the melt. On the other hand, the mixed difference scheme satisfies the pre-

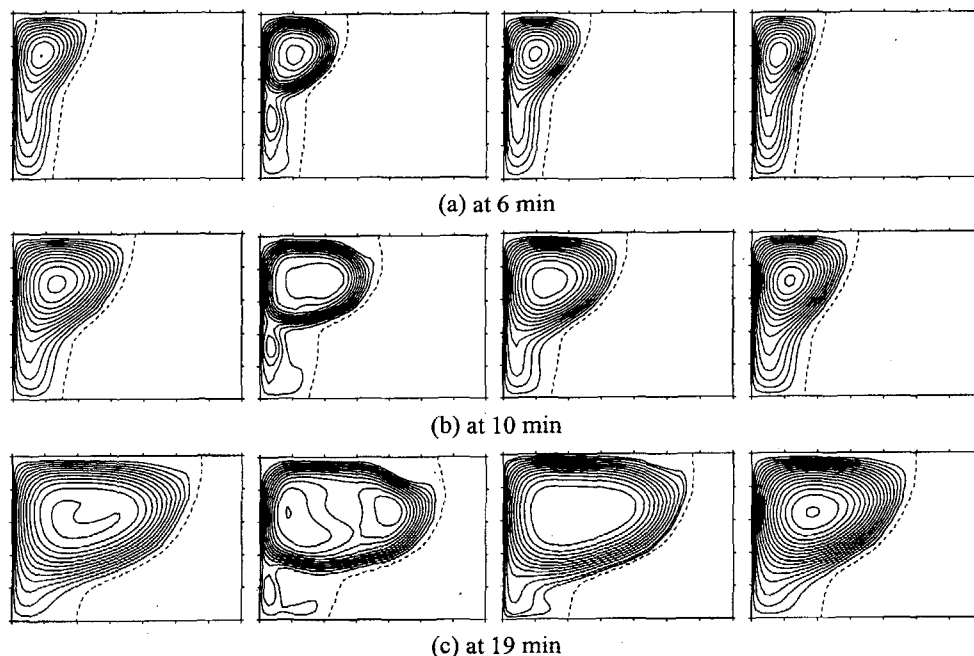


Fig. 3. Streamlines for gallium melting (from the left to the right, the upwind difference, the central difference, the mixed schemes and the power scheme).

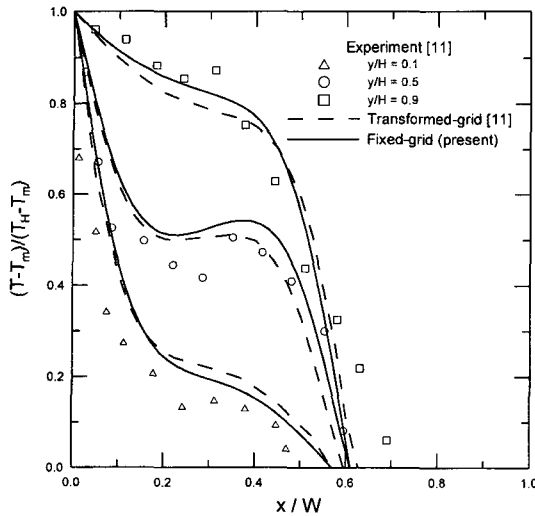


Fig. 4. Temperature distribution in the liquid during the solidification of tin at 0.529 hr.

dictability of the phase front and the flow structure in the melt, while the central difference scheme results in some distortion of the front as shown in Fig. 3 but not observed in the experiment.

The solidification of tin is also simulated with the proposed model. The experimental and the transformed-grid results by Wolff and Viskanta<sup>[11]</sup> shown in Fig. 1(b) are cited for the comparison. The major dimensionless numbers are  $Pr=0.0149$ ,  $Ra=6.794 \times 10^4$  and  $Ste=0.004807$ .

Figure 4 shows the temperature distribution in the liquid during the solidification of tin at 0.529 hr. The present fixed-grid solutions are very similar to the transformed-grid results. Considering some of the scatter in the measured temperatures as noted by Wolff and Viskanta,<sup>[11]</sup> the results generated from numerical methods are in fairly good agreement with the experimental data.

## 5. Conclusion

The convection-dominated melting and solidification in a rectangular cavity is investigated numerically on the basis of the fixed-grid formulation. The phase change process and the velocity suppression is modeled by the enthalpy-porosity method.

The gallium melting is simulated with the present model and the results are comparable with the exper-

imental data in the literature. The comparison with the transformed-grid calculation shows that the present model produces similar or better predictions of the macroscopic feature of the melting like the movement of the phase change front. The present model is verified with the experiment of the tin solidification and is also compared with the transformed-grid simulation.

The flow structure in the melt is investigated with various interpolation schemes for the convection term. The deferred correction scheme and the power scheme are tested. The usual upwind difference scheme and the power scheme fail to reproduce the detailed flow structure in the melt. The central difference scheme is able to predict the minor structure in the melt, but it somewhat distorts the phase front. On the contrary, the mixed difference scheme can simulate the detailed flow structure as well as the macroscopic behavior during phase change such as the front movement and the temperature distribution.

## References

1. Viswanath, R. and Jaluria, Y.: "A Comparison of Different Solution Methodologies for Melting and Solidification Problems," *Numer. Heat Transfer B Fund.*, 24, 77 (1993).
2. Patankar, S.V.: *Numerical Heat Transfer and Fluid Flow*, Hemisphere, Washington (1980).
3. Ferziger, J.H. and Peric, M.: *Computational Methods for Fluid Dynamics*, Springer, Germany (1999).
4. Kim, S., Kim, M.-C. and Lee, S.-B.: "Prediction of Melting Process Driven by Conduction-Convection in a Cavity Heated from the Side," *Korean J. Chem. Eng.*, 18, 593 (2001).
5. Gau, C. and Viskanta, R.: "Melting and Solidification of a Pure Metal on a Vertical Wall," *J. Heat Transfer Trans. ASME*, 108, 174 (1986).
6. Desai, C.P. and Vafai, K.: "A Unified Examination of the Melting Process within a Two-Dimensional Rectangular Cavity," *J. Heat Transfer Trans. ASME*, 115, 1072 (1993).
7. Brent, A.D., Voller, V.R. and Reid, K.J.: "Enthalpy-Porosity Technique for Modeling Convection-Diffusion Phase Change: Application to the Melting of a Pure Metal," *Numer. Heat Transfer*, 13, 297 (1988).
8. Beckermann, C. and Viskanta, R.: "Effect of Solid Subcooling on Natural Convection Melting of a Pure Metal," *J. Heat Transfer Trans. ASME*, 111, 416

- (1989).
9. Lacroix, M. and Voller, V.R.: "Finite Difference Solutions of Solidification Phase Change Problems: Transformed versus Fixed Grids," *Numer. Heat Transfer B Fund.*, 17, 25 (1990).
  10. Voller, V.R.: "An Overview of Numerical Methods for Solving Phase Change Problems," in *Advanced Numerical Heat Transfer* edited by Minkowycz, W.J. and Sparrow, E.M., 1, 341 (1997).
  11. Wolff, F. and Viskanta, R.: "Solidification of a Pure Metal at a Vertical Wall in the Presence of Liquid Superheat," *Int. J. Heat Mass Transfer*, 31, 1735 (1988).